Journal of Thermal Analysis and Calorimetry
https://doi.org/10.1007/s10973-020-09590-2

Comparative performance assessment of different absorber tube geometries for parabolic trough solar collector using nanofluid

Muhammad Sajid Khan[1,2] · Mi Yan[1] · Hafiz Muhammad Ali[3] · Khuram Pervez Amber[2] · Muhammad Anser Bashir[2] · Bilal Akbar[2] · Samina Javed[4]

Received: 8 October 2019 / Accepted: 17 March 2020

Abstract

Parabolic trough collector is the most mature and widely deployed concentrated solar power technology with temperature ranging from 325 to 700 K. In this study, three different absorber tube geometries (smooth absorber tube, absorber tube with twisted tape insert and tube with longitudinal fins) of commercially available LS-2 collector are modeled and investigated using engineering equation solver. The objective of this study is to present a numerical comparative analysis of the available thermal enhancement techniques. Comprehensive energetic and exergetic performance of different tube geometry configurations using Al_2O_3/water as a heat transfer fluid has been compared to assess the nature of exergy destruction due to the fluid's pressure, due to the heat transfer between sun and the receiver wall and due to the temperature difference between receiver wall and heat transfer fluid temperature. Furthermore, pure base fluid (water) along with the nanofluid is used to evaluate the system's performance (thermal efficiency, exergetic efficiency, heat transfer coefficient, receiver temperature, pressure drop, pumping work demand and friction factor). Smooth absorber tube with pure base fluid is the reference case, while five cases (smooth tube with nanofluid, tube with pure water and fins inserted, tube with nanofluid and fins inserted, tube with pure water and twisted tape inserted, tube with nanofluid and twisted tape inserted) are investigated. Thermal efficiency of absorber tube with twisted tape insert and nanofluid is almost 72.26%, followed by tube with internal fins (72.10%), while smooth absorber tube has nearly 71.09%. Heat transfer coefficient of twisted tape inserted tube with nanofluid and longitudinal fins tube with nanofluid is greater than smooth absorber tube to almost 118.23% and 103.26%, respectively. The emphasis is also given to the pressure drop of the examined cases as it depends up on the friction factor of the absorber tubes. The use of nanofluid and twisted tape inserts leads to higher thermal enhancement, followed by the nanofluid and internal fins inserted tube. The nanoparticle concentration is also varied to investigate its effect on different performance parameters of the system.

Keywords Parabolic trough · Absorber · Twisted tape · Longitudinal fins · Nanofluid · Base fluid · Thermal enhancement techniques · Turbulators

✉ Hafiz Muhammad Ali
hafiz.ali@kfupm.edu.sa

[1] Institute of Energy and Power Engineering, Zhejiang University of Technology, Hangzhou 310014, Zhejiang, China

[2] Department of Mechanical Engineering, Mirpur University of Science and Technology (MUST), Mirpur, AJK 10250, Pakistan

[3] Mechanical Engineering Department, King Fahd University of Petroleum & Minerals (KFUPM), Dhahran 31261, Saudi Arabia

[4] Department of Mechanical Engineering, Air University, Islamabad, Pakistan

List of symbols

A_{ap}	Aperture area (m^2)
A_r	Receiver area (m^2)
C_p	Specific heat capacity ($J\ kg^{-1}\ K^{-1}$)
$D_{c,o}$	Outer cover diameter (m)
$D_{r,o}$	Outer receiver diameter (m)
$\dot{E}_{X,Col}$	Collector exergy rate (W)
G_b	Solar radiation ($W\ m^{-2}$)
f	Friction factor
h	Heat transfer coefficient ($W\ m^{-2}\ K^{-1}$)
k_{nf}	Thermal conductivity of nanofluid ($W\ m^{-2}\ K^{-1}$)
T_c	Cover temperature (K)
T_a	Ambient temperature (K)
U_L	Coefficient of heat loss ($W\ m^{-2}\ K^{-1}$)
U_0	Overall heat transfer coefficient
$\dot{Q}_{loss}$	Heat loss (W)

Published online: 28 March 2020

$\dot{Q}_u$ Useful heat (W)
F_R Heat removal factor
$\dot{m}_r$ Mass flow rate (kg s^{-1})
$\dot{S}_{Gen}$ Entropy generation
B_{Num} Bejan number

Greek letters

ρ_{nf} Density of nanofluid (kg m^{-3})
μ_{nf} Dynamic viscosity
σ Stefan–Boltzmann constant
ε_{cv} Cover emissivity
φ Volumetric fraction of nanoparticle (%)
η_{en} Energy efficiency
η_X Exergy efficiency

Introduction

The utilization of solar energy is the most important way to tackle the severe energy problems that have been created due to the burning of fossil fuels [1, 2]. Concentrating solar power (CSP) plants are the most promising technologies to meet the energy demands, domestic and industrial heating, electricity generation, cooling and chemical processing [3, 4]. The CSP technologies include parabolic dish collector (PDC), parabolic trough collector (PTC), central tower with heliostat field and Fresnel lens. PTC is the most deployed and oldest technology among all above-mentioned technologies, with large number of applications [5]. It can gain temperature easily up to 800 K, with higher thermal efficiency and a reasonable cost [5–7].

Parabolic trough collector is the most mature and widely deployed CSP technology among all other technologies [8, 9]. It is low cost technology, temperature ranging from 325 to 700 K and can be used for variety of applications [10]. It consists of two parts, solar collector with parabolic shape and an evacuated receiver tube. It is more reliable than the other concentrating solar collectors as thermal losses from evacuated tube are less compared to the other available conventional technologies [10]. There are many researchers, who made their efforts to improve the heat transfer enhancement in the absorber tube. This purpose can be achieved by increasing the convection heat transfer coefficient and increase in the area of convection surface [11]. The convection heat transfer depends upon the heat transfer fluid, whereas turbulators or modifications used in the internal flow path are associated with the increase in the surface area of the receiver tube.

The mostly used heat transfer fluids in PTC are thermal oil, water, molten salts and gaseous working fluids [4]. The usage of direct steam generation power plants is limited due to the need for higher operating temperature level. Thermal oil can also be used as a heat transfer fluid (HTF) in PTC, and they can operate up to 675 K [12], but they have lower thermal performance as compared to the other heat transfer fluids. The use of molten salts and pressurized gases in PTC is a new trend for higher temperature applications. Molten salts are normally the nitrate salts that can easily gained up to 775 K [11]. However, their use required safety in operation due to their freezing danger if operating temperature is in between 373 and 505 K [13]. Pressurized gases can be able to get higher temperature level; especially, s-CO_2 has better thermophysical properties near critical point [14].

Many researchers have examined the utilization of nanofluids in the absorber tubes of PTC. These heat transfer fluids can be prepared by dispersion of metallic non-particles in base fluid, and this term was proposed by Choi and Eastman [15]. Basbous et al. [16] numerically investigated four different Syltherm 800-based nanofluids in PTC, and sufficient increase in heat transfer enhancement was found. Bellos et al. [10] examined CFD modeling of PTC (converging–diverging absorber tube) using AL_2O_3/thermal oil. The results showed that increase in thermal efficiency, heat transfer coefficient and pressure drop was almost 4.25%, 11% and 10%, accordingly. Numerical simulation of PTC using six different water-based nanofluids was investigated by Coccia et al. [17].

The use of turbulators and internal modifications/internal fins of absorber tubes in PTC is another technique for the augmentation of heat transfer. The twisted tape insert in the flow path of the absorber tube is the best available technique for heat transfer enhancement. Ghadirijafarbeigloo et al. [18] numerically examined the effect of Louvered twisted tape inserts in the receiver tube of PTC using Behran oil as a heat transfer fluid. Heat transfer coefficient and pressure drop were noticed to be increased significantly as compared to the plain twisted tape inserts. Jaramillo et al. [19] developed a thermodynamic model to investigate the performance of PTC with twisted tape insert using water as a heat transfer fluid. Increase in thermal efficiency was obtained almost, 25%. Some other researchers [20–22]

also used wall detached twisted tape, serrated twisted tape and wire coil in the tubes of PTC to examine heat transfer enhancement. Porous disks and rings were also analyzed numerically in the tubes of PTC by researchers [23, 24]. The internal geometrical modifications of the absorber tubes also led to the heat transfer enhancements but lower than the inserts. However, pressure drop was less in second case. Some researchers tried to modify the absorber tubes using fins in the lower part as studied by [25], porous fins [26] and the implication of longitudinal vortex generators [27]. Their results indicated very low heat transfer enhancement. The use of longitudinal fins and helical fins in the periphery of absorber tubes was examined by Bellos et al. [28] and Munoz and Abanades [29], respectively.

The aim of the present study is to investigate the heat transfer enhancement and pressure drop in the different absorber tubes of parabolic trough collector. Thermal enhancement methods will be carried out using turbulators in the flow paths, as it enhances the coefficient of heat transfer between fluid flow and the absorber tube. In other words, turbulence intensity can be enhanced by increasing the mixing of the fluid that further increases the thermal conductivity of the heat transfer fluid. The other method to increase the heat transfer coefficient is the use of nanofluids. As, our main goal will be to obtain higher thermal efficiency that is achieved at lower receiver temperature with less thermal losses. Due to the higher thermal conductivity and density of the nanofluids compared to the base fluids, nanofluids are the best heat augmentation fluids for application in the tubes of parabolic trough collector. The proposed study is conducted using Al_2O_3-/water-based nanofluid and pure base fluid (water) as a heat transfer fluid in the absorber tubes. The examined cases are used in the following sequence throughout the whole text:

Case 0 or reference case: Smooth tube with base fluid.
Case 1: Smooth tube with nanofluid.
Case 2: Internal fins inserted tube with base fluid.
Case 3: Internal fins inserted tube with nanofluid.
Case 4: Tube with twisted tape inserted and base fluid.
Case 5: Tube with twisted tape inserted and nanofluid.

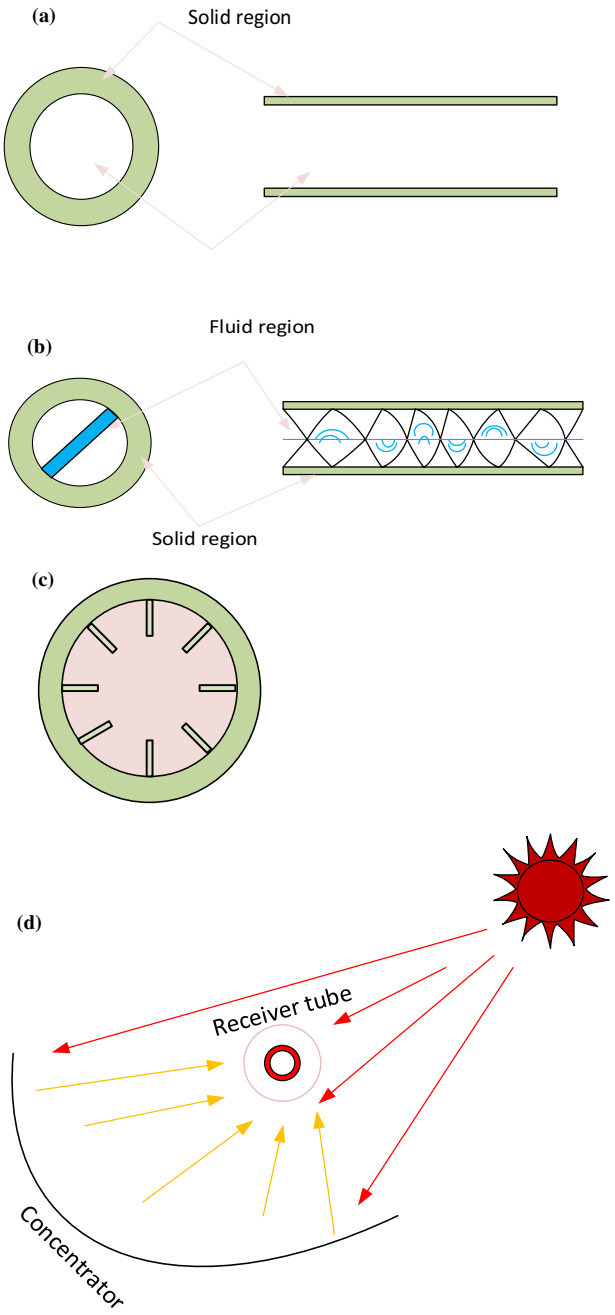

Fig. 1 Schematic description of **a** smooth absorber tube, **b** absorber tube with twisted tape insert, **c** absorber tube with internal fins and **d** two-dimensional cross-sectional view of the PTC system

System description

Figure 1a–c represents the longitudinal and cross section view of absorber tubes (smooth, tube with twisted tape insert and tube with internal helical fins, respectively) used in parabolic trough solar collector. Figure 1d is the two-dimensional cross-sectional view of the solar parabolic trough collector. The solar radiations fall on the reflective sheet and reflect to the absorber tubes. Heat is transferred to the fluid circulating inside absorber tubes. The parabolic trough model used in the present study is modeled after Sandia National Laboratory (SNEL) [30] LS-2 collector, and dimensions are given in Table 1. The receiver is coated with a selective absorptive material and made up of stainless steel.

Thermal analysis and methodology

This section presents detailed equations applied for the energy and exergy balance of the system. Mathematical model of parabolic trough collector with different absorber tubes using nanofluid and base fluid has been modeled in engineering equation solver based on parameters listed in Table 1. Assumptions are as follows:

- Steady state conditions are applied.
- Ambient temperature and atmospheric pressure are taken as 300 K and 101 kPa.
- Uniform heat flux in the simulation.

The aperture area and receiver area of trough collector can be calculated as:

$$A_{\mathrm{ap}} = L\left(W - D_{\mathrm{c,o}}\right). \tag{1}$$

$$A_{\mathrm{r}} = \pi L D_{\mathrm{r,o}}. \tag{2}$$

Here, W and L are the width and length of the collector and $D_{\mathrm{c,o}}$ and $D_{\mathrm{r,o}}$ represent outer cover and receiver diameters, respectively. To find the wind convection coefficient, Reynolds number is required to be calculated as suggested by Kalogiru [8].

$$R_{\mathrm{e}} = \frac{\rho V D_{\mathrm{c,o}}}{\mu} \tag{3}$$

where ρ is the density of the wind outside solar trough collector and μ is the dynamic viscosity. Reynolds number is further used to calculate Nusselt number.

For $1000 < R_{\mathrm{e}} < 50{,}000$,

$$N_{\mathrm{U,\,air}} = 0.3 R_{\mathrm{e}}^{0.6} \tag{4}$$

And for $0.1 < R_{\mathrm{e}} < 1000$,

$$N_{\mathrm{U,\,air}} = 0.4 + 0.54 R_{\mathrm{e}}^{0.52}. \tag{5}$$

It is required to calculate coefficients of heat transfer outside and inside collector prior to find out collector losses (U_{L}) and overall heat transfer coefficient (U_{o}). The convection heat transfer of wind outside the receiver can be calculated as:

$$h_{\mathrm{c,ca}} = \left(\frac{N_{\mathrm{u,air}} K_{\mathrm{air}}}{D_{\mathrm{co}}}\right). \tag{6}$$

Equation (7) is used to calculate the radiation of coefficient of heat transfer between environment and glass cover.

$$h_{\mathrm{r,ca}} = \sigma \varepsilon_{\mathrm{cv}} \left(T_{\mathrm{c}} + T_{\mathrm{a}}\right)\left(T_{\mathrm{c}}^2 + T_{\mathrm{a}}^2\right) \tag{7}$$

where σ is Boltzmann constant and $\varepsilon_{\mathrm{cv}}$ represents glass cover emissivity

Another relation to find radiation heat transfer coefficient between glass cover and receiver can be computed using Eq. (8).

$$h_{\mathrm{r,cr}} = \frac{\sigma\left(T_{\mathrm{c}} + T_{\mathrm{r,av}}\right)\left(T_{\mathrm{c}}^2 + T_{\mathrm{r,av}}^2\right)}{\frac{1}{\varepsilon_{\mathrm{r}}} + \frac{A_{\mathrm{r}}}{A_{\mathrm{c}}}\left(\frac{1}{\varepsilon_{\mathrm{cv}}} - 1\right)}. \tag{8}$$

Overall heat loss coefficient through collector that based on receiver area is depicted in Eq. (9).

$$U_{\mathrm{L}} = \left[\frac{A_{\mathrm{r}}}{\left(h_{\mathrm{c,ca}} + h_{\mathrm{r,ca}}\right)A_{\mathrm{c}}} + \frac{1}{h_{\mathrm{r,cr}}}\right]^{-1}. \tag{9}$$

Table 1 Characteristics of the LS-2 parabolic trough solar collector [30]

Manufacturer	Luz industrial
Module size	7.8 m×5m
Collector reflectance	0.935
Aperture area	39.2 m^2
Concentration ratio	22.74
Outer diameter of the glass cover	115 mm
Inner diameter of the glass cover	109 mm
Transmittance of the glass cover	0.95
Absorptivity of absorber tube	0.96
Inner diameter of absorber tube	66 mm
Outer diameter of tube	70 mm
Optical efficiency	75.5%
Emittance of cover	0.86

Another expression to calculate heat loss coefficient is associated with t thermal losses.

$$U_L = \frac{\dot{Q}_{loss}}{A_r(T_r - T_a)}. \tag{10}$$

Heat removal factor is the ratio between useful heat gain actual and fluid's inlet temperature.

$$F_R = \frac{\dot{m}_r Cp_r}{A_r U_L}\left[1 - \exp\left(\frac{-A_r U_L F_1}{\dot{m}_r Cp_r}\right)\right] \tag{11}$$

where $\dot{m}_r$ is the mass flow rate through collector.

The useful heat gain through collector and glass cover temperature can be found as:

$$\dot{Q}_u = A_{ap}F_R\left(S - \frac{A_r}{A_{ap}}U_L(T_{ri} - T_0)\right) \tag{12}$$

$$\dot{Q}_u = A_{ap}F_R\left(S - \frac{A_r}{A_{ap}}U_L(T_{ri} - T_0)\right) \tag{13}$$

where S is the absorbed solar radiations ($S = G_b\eta_O$)

The rate of solar energy available is given as:

$$\dot{Q}_{solar} = A_{ap}F_R S. \tag{14}$$

Now, the overall coefficient of heat transfer through the collector is computed as:

$$U_o = \left[\frac{1}{U_L} + \frac{D_{r,o}}{h_{c,r,in\,D_{r,i}}} + \left(\frac{D_{r,o}}{2K_r}\ln\frac{D_{r,o}}{D_{r,i}}\right)\right]^{-1}. \tag{15}$$

K_r in the above equation is the thermal conductivity of receiver tube.

The performance of the parabolic trough solar collector will be attributed on the fact of how efficiently solar collector converts energy of sun into useful thermal energy and given by:

$$\eta_{en,PTSC} = F_r\left[\eta_O - U_L\left(\frac{T_{r,i} - T_a}{G_b C}\right)\right]. \tag{16}$$

Analysis of flow in smooth absorber tube

The smooth absorber tube shown in Fig. 1a is used as a reference case. The useful energy is transferred from the walls of the receiver tube to the fluid circulating in it by means of convection. The nature of this fluid is turbulent within the absorber tube. A correlation is developed by Gnielinski [31] to calculate Nusselt number in the turbulent and transition region.

$$N_u = \frac{\left(\frac{f}{8}\right)P_r(R_{eD} - 1000)}{1 + 12.7\left(\frac{f}{8}\right)^{\frac{1}{2}}\left(P_r^{\frac{2}{3}} - 1\right)}. \tag{17}$$

Petukhov correlation [32] will be used for the value of friction factor.

$$f = (0.790\ln \mathrm{Re} - 1.64)^{-2} \tag{18}$$

$$\Delta P = f\frac{L}{D_{r,i}}\left(\frac{1}{2}\frac{\rho\mu^2}{1}\right). \tag{19}$$

Absorber tube with internal fins

For internally finned tube, a conventional smooth tube is modified to have longitudinal rectangular fins as shown in Fig. 1c. The fins enhance the heat transfer rate through the absorber tube. The presence of fins increases the effective thermal conductivity of the heat transfer fluid by reducing the circumferential temperature. The relationship used to calculate the pressure drop and heat transfer within the internally finned absorber tube has been suggested by Bellos et al. [33].

$$N_{\mathrm{u,\,FT}} = 0.01638\mathrm{Re}^{0.851}P_{\mathrm{r}}^{0.374}\left[1 + 0.4442\left(\frac{t}{D_{\mathrm{r,i}}}\right)^{0.270}\left(\frac{p}{D_{\mathrm{r,i}}}\right)^{1.024}\right]. \tag{20}$$

Furthermore, friction factor for such absorber tubes can be calculated as:

$$f_{\mathrm{FT}} = \frac{0.2585}{\mathrm{Re}^{0.2386}}\left[1 + 2.7452\left(\frac{t}{D_{\mathrm{r,i}}}\right)^{0.118}\left(\frac{p}{D_{\mathrm{r,i}}}\right)^{0.839} \cdot \exp\left(9.711\frac{t}{D_{\mathrm{r,i}}}\right) \cdot \exp\left(4.010\frac{p}{D_{\mathrm{r,i}}}\right)\right]. \tag{21}$$

In the present study, fin height p and pitch length t for the suggested model design are taken as 10 mm and 2 mm, respectively.

Absorber tube with twisted tape inserts

The third case discussed in the present study is the twisted tape insert in an empty absorber tube (Fig. 1b). Tapes are made of aluminum strips and inserted in such a way to have a sufficient contact with the receiver walls. The swirls produce more turbulence due to the twisted tape inserts. The twisted tape is supposed to enhance the rate of heat removal from the tube to supply more heat (useful) to the heat transfer fluid. Pressure drop and Nusselt number of the tubes with twisted tape insert are calculated by the correlation presented by Jaramillo et al. [19].

$$N_{\mathrm{u,\,TT}} = 0.224\mathrm{Re}^{0.66}P_{\mathrm{r}}^{0.4}\left(\frac{y}{w}\right)^{-0.6} \tag{22}$$

$$f_{\mathrm{FT}} = 65.4\mathrm{Re}^{-0.52}\left(\frac{y}{w}\right)^{-1.31} \tag{23}$$

where w and y are the tape width (diameter) and tape pitch length, respectively.

The volumetric flow rate through the absorber tube is expressed as:

$$V_{\mathrm{f}} = 60,000.u.A_{\mathrm{ri}} \tag{24}$$

where u is the velocity of fluid flow inside tube.

Second law analysis

Second law analysis is an important parameter that measures the actual performance of the receiver collector. Exergy efficiency of parabolic trough collector is the ratio of heat exergy of the receiver to the available solar thermal exergy.

$$\eta_{\mathrm{X,PTSC}} = \frac{\dot{E}_{\mathrm{X,\,Col}}}{\dot{E}_{\mathrm{X,\,solar}}}. \tag{25}$$

Exergy of collector and exergy of solar can be described by the following equations.

$$\dot{E}_{\mathrm{X,\,Col}} = \dot{Q}_{\mathrm{prod}}\left(1 - \frac{T_{\mathrm{a}}}{T_{\mathrm{avg}}}\right) \tag{26}$$

$$\dot{E}_{\mathrm{x,\,solar}} = G_{\mathrm{b}} \cdot A_{\mathrm{a}} \cdot \eta_{\mathrm{pet}} \tag{27a}$$

$$\eta_{\mathrm{pet}} = 1 - \frac{4T_0}{3T_{\mathrm{sun}}} + \frac{1}{3}\left(\frac{T_0}{T_{\mathrm{sun}}}\right)^4. \tag{27b}$$

To perform a comprehensive exergy analysis of the system, exergy destroyed and exergy losses in the system are important to understand. The destruction of exergy in the system represents the irreversibility, and it is due to the three factors: fluid's pressure drop through the receiver because of friction and can be modeled as:

$$\dot{E}_{\mathrm{X,\,des,\Delta p}} = T_{\mathrm{a}} \cdot \dot{m}_{\mathrm{r}} \cdot \frac{\Delta p \ln\left(\frac{T_{\mathrm{out}}}{T_{\mathrm{in}}}\right)}{\rho\left(T_{\mathrm{out}} - T_{\mathrm{in}}\right)}. \tag{28}$$

Now, the rate of exergy destroyed due to the temperature difference between receiver wall and sun temperature:

$$\dot{E}_{\mathrm{X,\,des,abs}} = \dot{m}_{\mathrm{r}}C_{\mathrm{p}}\left(T_{\mathrm{out}} - T_{\mathrm{in}}\right)T_{\mathrm{a}}\left(\frac{1}{T_{\mathrm{r}}} - \frac{1}{T_{\mathrm{sun}}}\right). \tag{29}$$

Destructed exergy rate due to the temperature difference between receiver wall and nanofluid is calculated as:

$$\dot{E}_{\mathrm{X,\,des,cond}} = \dot{m}_{\mathrm{r}}C_{\mathrm{p}}T_{\mathrm{a}}\left(\ln\frac{T_{\mathrm{out}}}{T_{\mathrm{in}}} - \frac{T_{\mathrm{out}} - T_{\mathrm{in}}}{T_{\mathrm{r}}}\right). \tag{30}$$

Total irreversibility is the sum of all the exergy destruction rates and given as:

$$\dot{E}_{\mathrm{X,\,des,tot}} = \dot{E}_{\mathrm{X,\,des,\Delta p}} + \dot{E}_{\mathrm{X,\,des,abs}} + \dot{E}_{\mathrm{X,\,des,cond}}. \tag{31}$$

Furthermore, the exergy losses or leakage exergy rate is due to the leakage of heat from receiver to the surroundings and due to the optical error.

$$\dot{E}_{\mathrm{X,\,loss}} = \dot{E}_{\mathrm{X,\,loss,opt}} + \dot{E}_{\mathrm{X,\,loss,ther}}. \tag{32}$$

Losses because of optical error can be determined as:

$$\dot{E}_{\mathrm{X,\,loss,opt}} = \left(1 - \eta_{\mathrm{O}}\right)\dot{E}_{\mathrm{X,\,solar}} \tag{33}$$

and thermal losses can be defined as:

$$\dot{E}_{\mathrm{X,\,loss,ther}} = \dot{Q}_{\mathrm{loss}} \left(1 - \frac{T_{\mathrm{a}}}{T_{\mathrm{r}}}\right). \tag{34}$$

Entropy generation of the proposed examined system can be summarized as:

$$\dot{S}_{\mathrm{Gen}} = \frac{\dot{E}_{\mathrm{X,\,loss}} + \dot{E}_{\mathrm{X,\,des,tot}}}{T_{\mathrm{a}}}. \tag{35}$$

Bejan number is the ratio between entropy generation because of the heat transfer and total entropy generation [34].

$$B_{\mathrm{Num}} = \frac{\dot{S}_{\mathrm{Gen\,,\,HT}}}{\dot{S}_{\mathrm{Gen}}} \tag{36}$$

$$\dot{S}_{\mathrm{Gen,\,HT}} = \frac{\dot{E}_{\mathrm{X,loss}} + \dot{E}_{\mathrm{X,\,des,abs}} + \dot{E}_{\mathrm{X,\,des,cond}}}{T_{\mathrm{a}}}. \tag{37}$$

Nanofluids properties

The heat transfer fluids used in the present study are the Al_2O_3-/water-based nanofluid and pure base fluid. Due to the higher thermophysical properties of the nanofluids compared to the base fluids, nanofluids are being selected for the heat transfer enhancement purpose [35].

The density and specific heat capacity of nanofluids can be calculated using the relations given below.

$$\rho_{\mathrm{nf}} = \rho_{\mathrm{bf}} \cdot (1 - \varphi) + \rho_{\mathrm{np}} \cdot \varphi \tag{38}$$

$$C_{\mathrm{p,nf}} = \frac{\rho_{\mathrm{bf}} \cdot (1 - \varphi)}{\rho_{\mathrm{nf}}} \cdot C_{\mathrm{p,bf}} + \frac{\rho_{\mathrm{np}} \cdot \varphi}{\rho_{\mathrm{np}}} \cdot C_{\mathrm{p,np}} \tag{39}$$

where ρ_{nf}, $C_{\mathrm{p,np}}$ and φ are the heat capacities of nanofluid, base fluid and nanoparticle's volumetric fraction (2% in the present study), respectively. Specific heat capacity is achieved by considering a thermal equilibrium state between base fluid and nanoparticles.

Thermal conductivity is calculated by Maxwell relation.

$$k_{\mathrm{nf}} = \frac{k_{\mathrm{np}} + 2 \cdot k_{\mathrm{bf}} - 2 \cdot \varphi \cdot \left(k_{\mathrm{bf}} - k_{\mathrm{np}}\right)}{\frac{k_{\mathrm{np}}}{k_{\mathrm{bf}}} + 2 + \frac{k_{\mathrm{bf}} - k_{\mathrm{np}}}{k_{\mathrm{bf}}} \cdot \varphi}. \tag{40}$$

The method proposed by Batchelor [36] is used to find the viscosity of nanofluids.

$$\mu_{\mathrm{nf}} = \mu_{\mathrm{bf}} \cdot \left(1 + 2.5 \cdot \varphi + 6.5 \cdot \varphi^2\right). \tag{41}$$

There are some additional parameters, which are essential to calculate such as Nusselt number, Reynolds number and Prandtl number. Convective heat transfer coefficient and convective heat transfer through the receiver depend on these parameters.

Reynolds number varies as the mass flow rate of heat transfer fluid inside the receiver will change as given by equation.

$$\mathrm{Re} = \frac{4 \cdot \dot{m}}{P_{\mathrm{cs}} \cdot \mu} \tag{42}$$

where P_{cs} is the perimeter of the inner part of the receiver tube. To find out the Nusselt number for turbulent regions, first Prandtl number has to be calculated using Eq. (43) and then convective heat transfer coefficient (h_{conv}).

$$\mathrm{Pr} = \frac{\mu_{\mathrm{nf}} \cdot C_{\mathrm{p,nf}}}{k_{\mathrm{nf}}} \tag{43}$$

$$h_{\mathrm{conv}} = \frac{\mathrm{Nu}_{\mathrm{nf}} \cdot k_{\mathrm{nf}}}{D_{\mathrm{h}}} \tag{44}$$

where D_{h} is the hydraulic diameter $\left(D_{\mathrm{h}} = \frac{4 \cdot A_{\mathrm{cs}}}{P_{\mathrm{cs}}}\right)$

The convective heat transfer through the nanofluids is calculated using the following relation.

$$Q_{\mathrm{conv}} = h_{\mathrm{conv}} \cdot A_{\mathrm{ri}} \left(T_{\mathrm{r}} - T_{\mathrm{avg}}\right) \tag{45}$$

where T_{r} and T_{avg} are the surface temperature of the receiver and average temperature of the heat transfer fluid, respectively.

Finally, minimum pumping work required in any case is given as:

$$W_{\mathrm{pump}} = \frac{m \cdot \Delta P}{\rho}. \tag{46}$$

Model validation

The validation for the nanofluid simulation is carried out using Eq. (17) in Fig. 2a, while Fig. 2b depicts the comparison of energy and exergy efficiencies between the present model and results from Bellos et al. [37]. In Fig. 7a, numerical results obtained through the simulation work are very close to the reference model with a mean deviation of 1.26%. The mean deviation of energy and exergy efficiency values between present model results and Bellos et al. [38] is 1.96% and 1.5%, respectively. Furthermore, Table 2 presents the validation of absorber outlet temperature of the smooth absorber tube (with nanofluid) with the experimental results of Dudely et al. [30]. Seven different operating conditions have been checked by varying the inlet temperature, while solar radiation and ambient temperature changed in a very

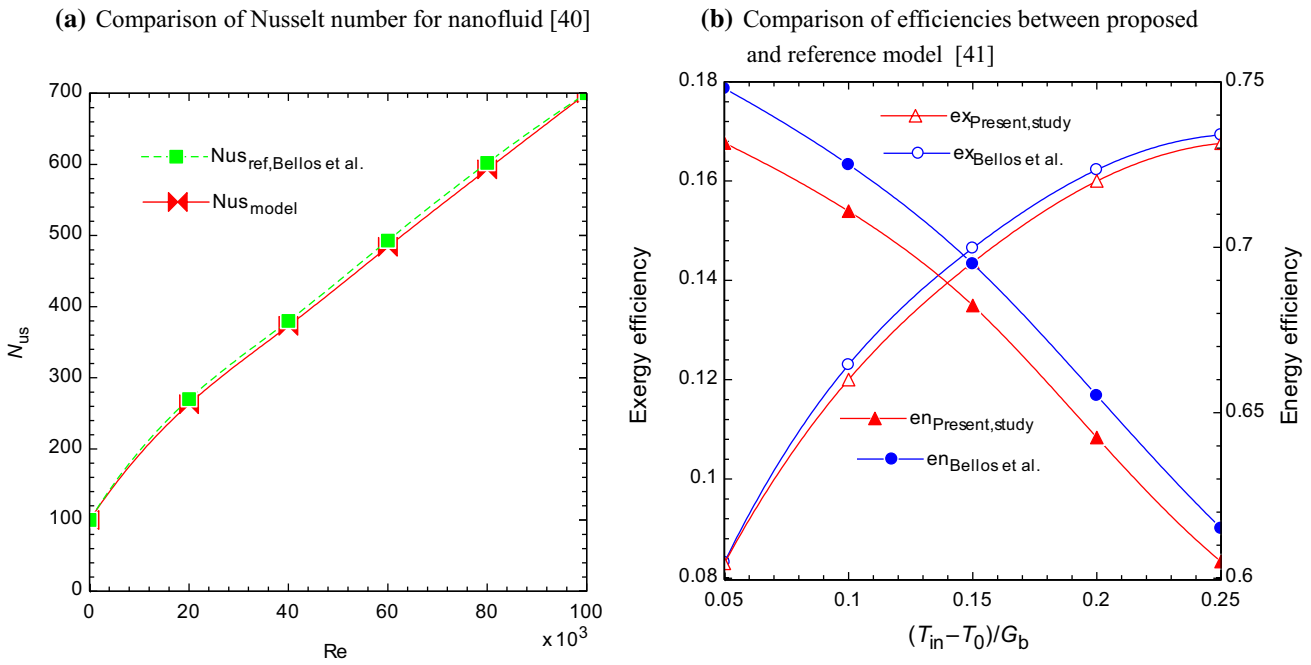

Fig. 2 **a** Comparison of Nusselt number for nanofluid [37]. **b** Comparison of efficiencies between proposed and reference model [38]

Table 2 Validation of the current developed model with Ref [30]

Cases	G_b/W/m^2	T_{am}/K	T_{in}/K	Outlet temperature		
				T_{out}/K		
				Ref [30]	Model	Deviation/%
1	934	294.4	375.4	397.2	397.35	0.038
2	968	295.6	424.4	446.5	446.9	0.09
3	982	297.5	470.7	492.7	493.1	0.081
4	910	299.5	523.9	542.6	542.85	0.046
5	938	299.4	571	589.6	589.9	0.050
6	881	302	572.2	590.4	590.1	0.051
7	903	300.7	629.1	647.2	646.95	0.038
Mean	–	–	–	–	–	0.056

less range. The mean deviation of the outlet temperature has been observed to almost 0.056%. These values are in acceptable range that proved the model validation.

Results and discussion

Parabolic trough solar collector with three different absorber tubes is modeled and compared for their exergy destructions, exergy losses, energy and exergy efficiencies, pressure drops, convective heat transfer coefficient, friction factor and receiver temperature. Five scenarios are discussed and compared with the reference case (smooth absorber tube with base fluid (water) as a heat transfer fluid). Thermodynamic modeling is conducted in engineering equation solver.

Figure 3a represents the influence of three different geometry configurations (nanofluid cases) on exergy destroyed due to the heat transfer between sun and receiver as well as between receiver wall and heat transfer fluid. Equations (29) and (30) illustrate the better explanation of Fig. 3a. Both the performance parameters are noticed to be reduced at higher values of inlet temperatures. The impact of higher fluid temperature decreases the receiver temperature, and incoming solar exergy is converted by the solar collector to the internal exergy of the heat transfer fluid. Figure 3b is the graphical representation of exergy destroyed due to the heat transfer fluid's pressure drop in the receiver of the three investigated

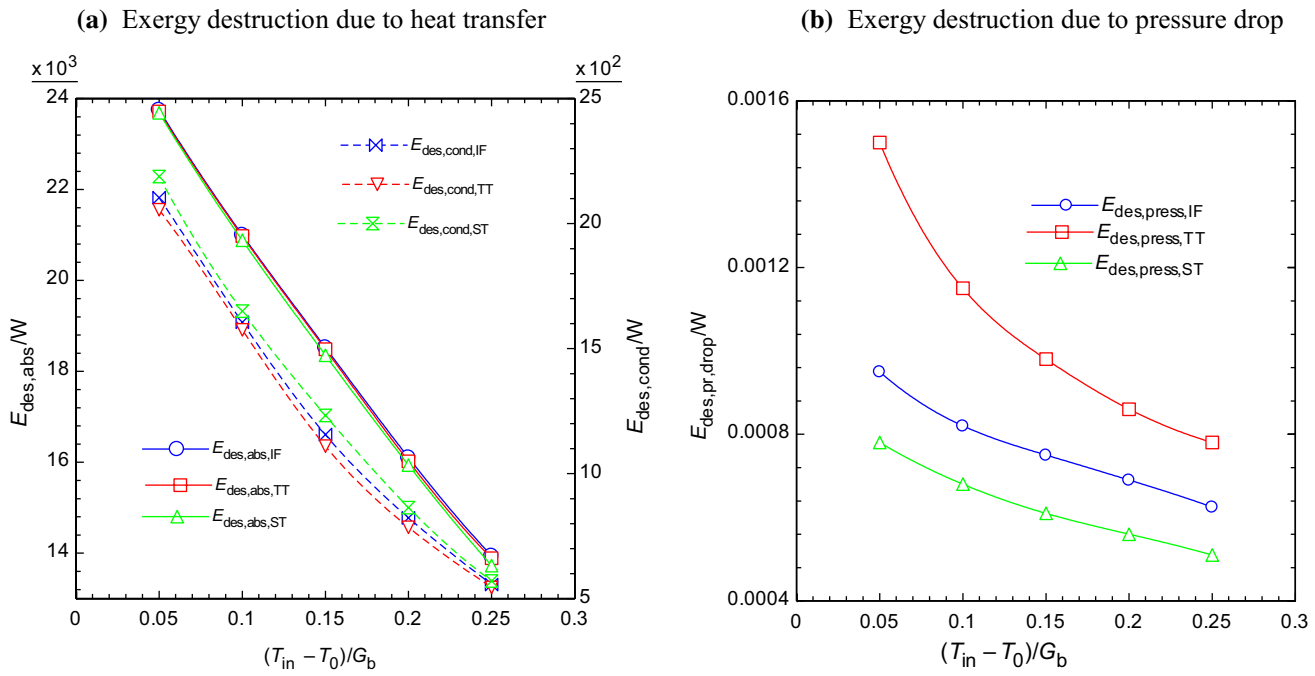

Fig. 3 **a** Exergy destruction due to heat transfer. **b** Exergy destruction due to pressure drop

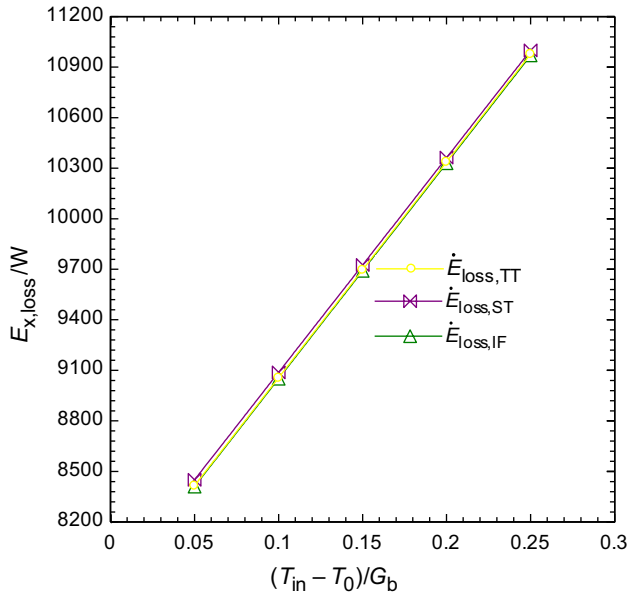

Fig. 4 Exergy losses of the three examined cases

cases (nanofluid cases). Absorber tube with twisted tape insert (case 5) has the highest value of exergy destruction because of pressure drop, and these values for all cases have decreasing trend by increasing the inlet temperature.

Equation (32) describes the overall exergy losses due to the optical and thermal losses, and its graphical representation is shown in Fig. 4. Smooth absorber tube (case 1) has the highest exergy losses, while twisted tape insert (case 5) has the better performance due to the turbulence and enhances swirls and it lowers the absorber tube's outer temperature. All the three considered cases (nanofluid cases) have same trend when evaluating against temperature, increase in exergy loss with rise in temperature.

Figure 5a shows the effect of varying inlet temperature on energetic efficiencies of the investigated system using three different absorber tube geometries with Al_2O_3/water and pure base fluid (water). Ambient temperature and solar radiation remain almost constant. The main reason for the use of various thermal augmentation techniques in parabolic trough absorber tube is to increase thermal efficiency. Rise in the inlet temperature gives lower thermal efficiency for all the cases, as receiver temperature gets higher with maximum thermal losses from the absorber surface. Case 5 has the best performance as compared to the other tube geometries for nanofluid and pure base fluid cases for all the examined temperatures. Case 5 has almost 74.15% thermal efficiency, and it is nearly 0.095% higher than case 3 and 1.36% case 1, respectively. The presence of twisted tapes generates more swirls and turbulence intensity by enhancing the mixing of heat transfer fluid and to rise the effective thermal conductivity of the fluid.

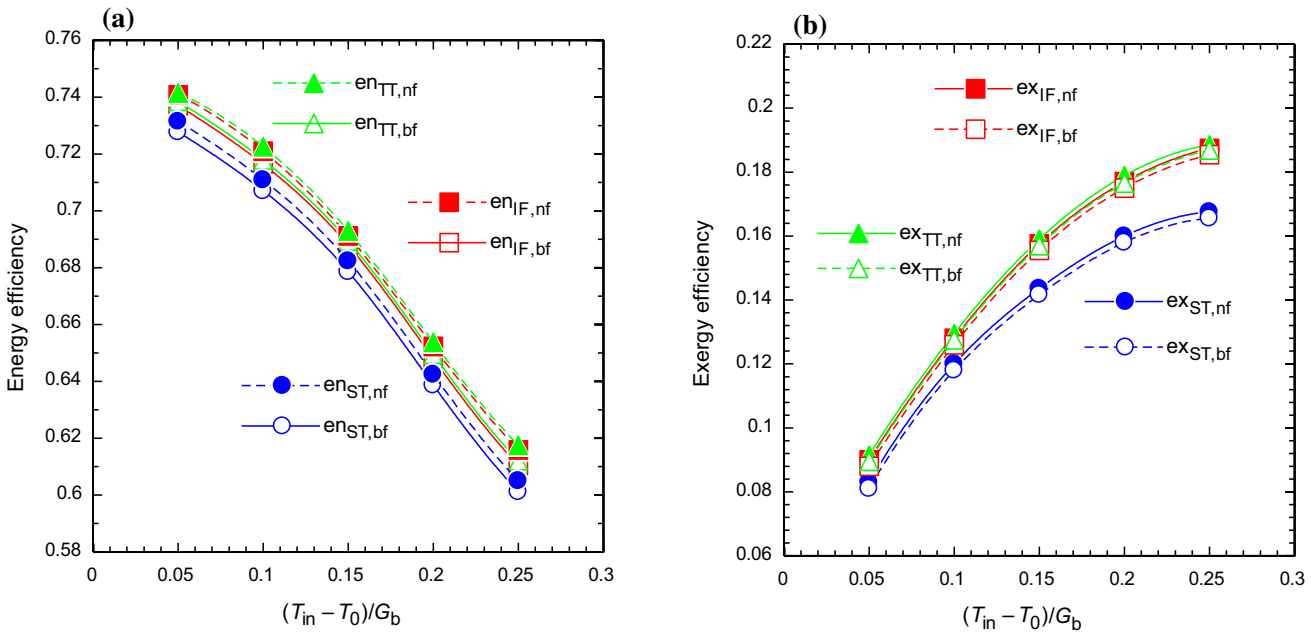

Fig. 5 **a** Comparison of energy efficiencies and **b** exergy efficiencies

Furthermore, Fig. 5b depicts the rise in exergy efficiencies of receiver tube against different inlet temperatures. At higher inlet temperatures, exergy efficiency has the maximum values in contrast to energy efficiency due to the increase in the available heat for useful exergy. Exergy efficiency of case 5 is almost 1.66% more than case 3, while 10.2% higher than case 1. The difference in the efficiency values is very less at lower inlet temperature, but after 400 K, the difference in the curve for cases 2, 3, 4 and 5 starts to increase. It is due to the thermal properties difference between nanofluid and base fluid. Exergy efficiency relies on the temperature rise of the working fluid, and higher outlet temperature means the maximum work production possibility.

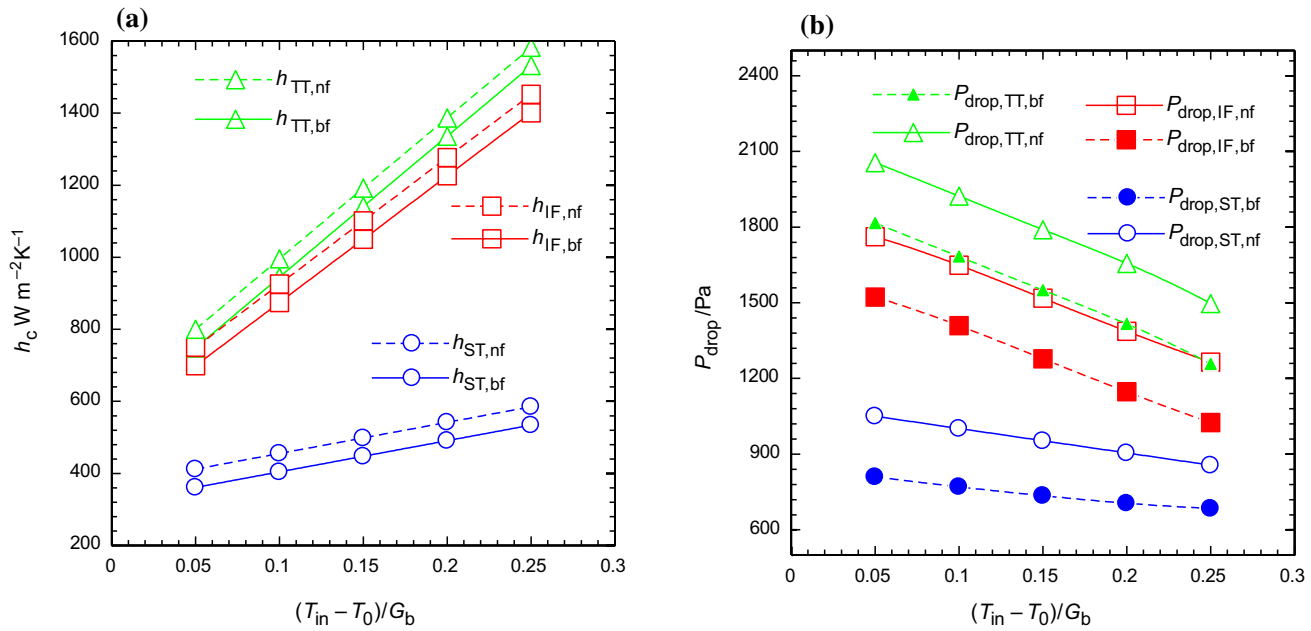

Fig. 6 **a** Comparison of heat transfer coefficient and **b** pressure drop

Figure 6a presents the convective heat transfer coefficient between working fluid and absorber for all the examined tube cases. It is the most crucial parameter in the present evaluation, as prime interest of the nanoparticle dispersion in the base fluid is to enhance this coefficient. Coefficient of heat transfer for case 5 has increased to almost 98% and case 3 increases to 93.6%, while 42% heat transfer coefficient is increased for case 1. The investigated performance parameter is maximum for nanofluid with twisted tape (case 5); therefore, the same case has higher thermal efficiency as compared to the other cases. Case 5 has approximately 6.67%, 6.80%, 14.45% and 94% higher heat transfer coefficient value from case 3, case 4, case 2 and case 1, respectively.

Pressure drop for all the examined cases is plotted against increase in the inlet temperature as seen in Fig. 6b. Higher-pressure drops are linked with the absorber tubes with greater enhancement in thermal efficiency. Higher heat transfer is related to the maximum pressure drop and it is a drawback of the thermal enhancement method as it directly associates with the pumping work and operating cost. Furthermore, higher inlet temperature corresponds to small pressure losses because dynamic viscosity is lower at higher inlet temperature levels. Case 5 shows the highest-pressure drop to almost 41%, while reference case has the least drop nearly 18%.

Figure 7a shows that the smooth absorber tube (reference case and case 1) has less friction factor as it has least pressure drop, while case 4 has the highest friction factor as compared to the other investigated cases. Increase in the inlet temperature reduces the pressure difference of the outlet and inlet pressure in the receiver tube. Dynamic viscosity of the fluid also decreases with rise in temperature so value of Reynolds number will be greater but corresponding friction factor inside the receiver tube is reduced. Therefore, higher inlet temperatures of fluid reduces the friction factor for all the considered cases.

Moreover, receiver temperature of all the considered cases is depicted in Fig. 7b. The obtained results present that less effective scenario according to the thermal efficient point of view shows higher receiver temperature (thermal losses increase with higher receiver temperatures) [37]. Generation of swirls in twisted tape inserted receiver tube (case 5) ensures a reliable mean temperature of the fluid, and it ultimately reduces the receiver outer temperature. Higher circumferential temperature of the receiver reduces the thermal efficiency.

Figure 8a is the graphical representation of pumping work in Watts required for the investigated cases to circulate the heat transfer fluid in the collector loop. This crucial parameter is associated with the flow friction as it also effects on the system operating cost. Case 5 (nanofluid and twisted tape) leads to the higher pumping work, while reference case and case 1 (smooth tubes with and without nanofluid) have the lowest pumping work required. Nanofluids increase the pumping work due to the rise in viscosity. The behavior of pumping work and pressure drop is almost very similar. For twisted tape absorber tube cases (case 5 and case 4), required pumping power is almost 174% and 152%, respectively, higher than the reference case. The amount of the pumping

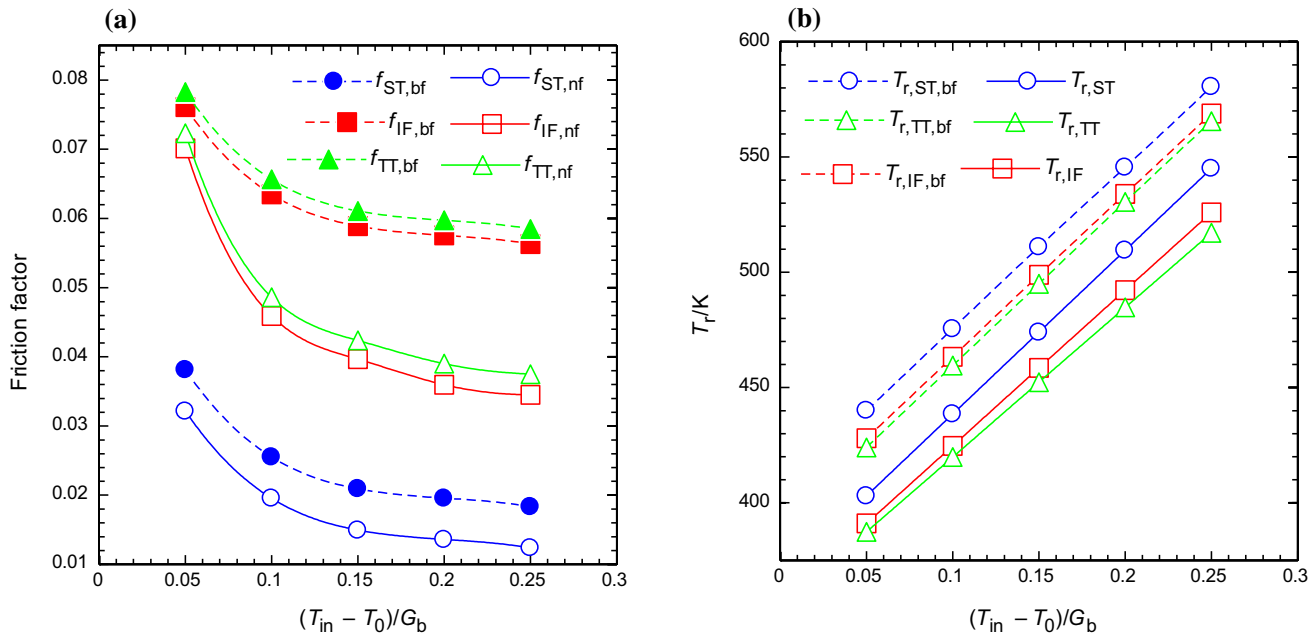

Fig. 7 **a** Comparison of friction Factor and **b** receiver temperature

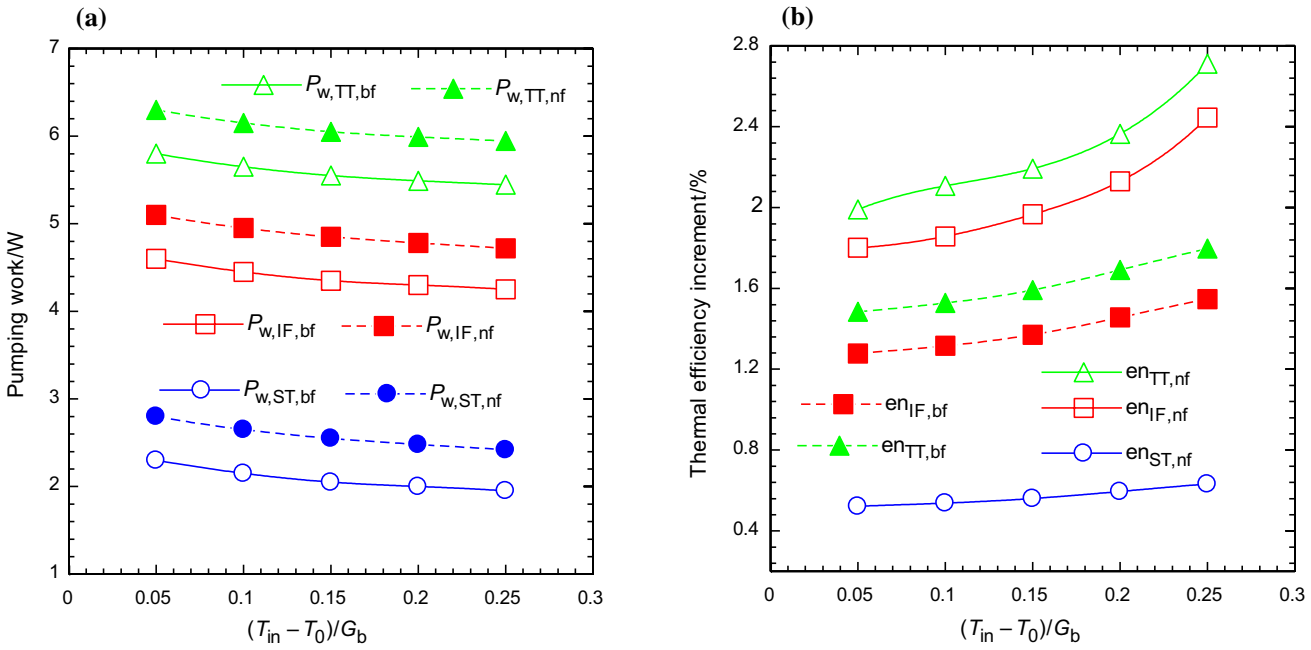

Fig. 8 **a** Comparison of pumping work demand and **b** thermal efficiency increase compared to the water-smooth case

work required is very low as compared to the solar input and useful heat production.

Figure 8b illustrates the enhancement in thermal efficiency using heat transfer enhancement techniques for the investigated inlet temperature ranges. Thermal efficiency enhancements are greater at higher temperature levels, an important point that PTCs usually operate at high temperature ranges. The thermal losses are maximum at these temperature ranges (higher inlet temperatures), so enhancement in thermal efficiency margin is greater [33]. Thermal efficiency enhancement using case 4 (base fluid with twisted tape) ranges from 1.48 to 1.79%, while case 2 (base fluid with fins) from 1.27 to 1.54%. However, the combination of nanofluid with twisted tape (case 5) and fins (case 3) gives 1.99% to 2.71% and 1.8% to 2.44%, respectively. The results of Fig. 8b clearly show that case 5 is the best scenario and technique for thermal enhancements as compared to the other cases.

The effect of inlet temperature on Bejan number for the three investigated cases is explained in Fig. 9. Bejan number is related to the entropy generation, while entropy generation depends on exergy losses and exergy destruction. Increasing the inlet temperature also rises the surface temperature of the absorber tube that will enhance the irreversibility. Finally, useful heat gain will be less. Smooth absorber tube has the highest rate of entropy generation due to the maximum receiver circumferential temperature that leads to the greatest Bejan number. However, lower Bejan number represents the higher thermal efficiency that is related to the twisted tape inserted tube (case 5).

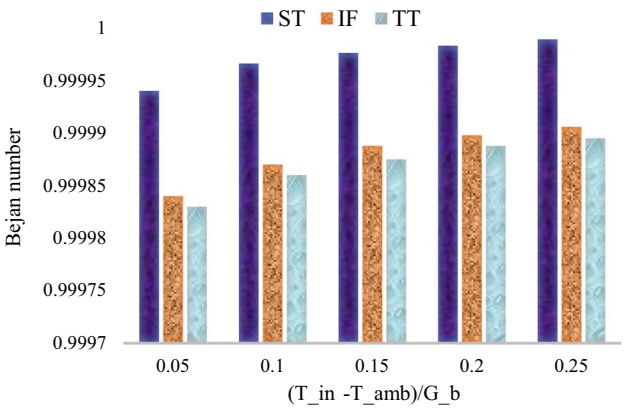

Fig. 9 Bejan number of the examined cases (nanofluid)

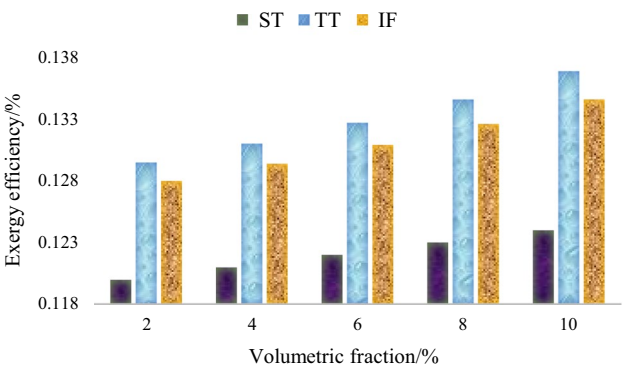

Fig. 10 Variation in exergy efficiency of the examined cases (nanofluid) at $T_{in} = 400$ K

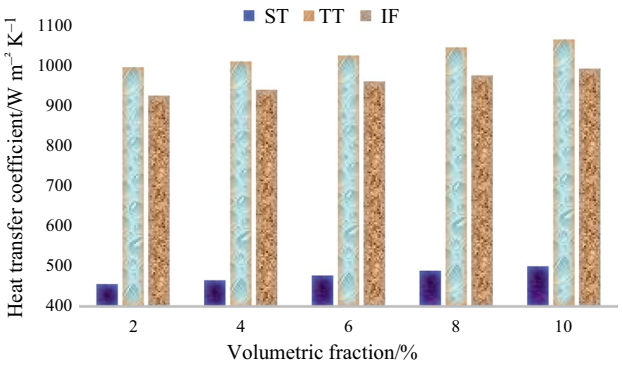

Fig. 13 Variation in heat transfer coefficient of the examined cases at $T_{in}=400$ K

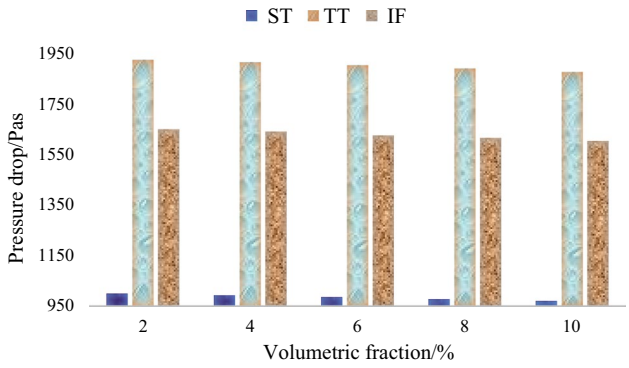

Fig. 12 Variation in pressure drop of the examined cases at $T_{in}=400$ K

Figures 10–13 show the results of exergy efficiency, receiver temperature, pressure drop and heat transfer coefficient, respectively, against change in the volumetric fraction of nanoparticles. It is clear that higher value of exergetic efficiency links to the higher concentration ratio of nanoparticle. Furthermore, tube with twisted tape insert (case 5) leads to the maximum efficiency as compared to the other investigated cases. More specifically, case 5 has improved to almost 5.71% followed by internal fin tube (case 3) to 5.01%; however, smooth tube (case 1) is only limited to 3.3% improvement.

Receiver surface temperature also varies with nanoparticle concentration as shown in Fig. 11. There is a slight increase in the temperature by enhancing the nanoparticle concentration for the three investigated cases. Absorber tube with twisted tape (case 5) has 0.28% increase in the receiver temperature, while other two have nearly 0.47% enhancement with increase in the nanoparticle concentration. The vortex or swirl inside the twisted tape inserted tube causes a better temperature distribution in the fluid flowing, further reducing the circumferential temperature of the receiver.

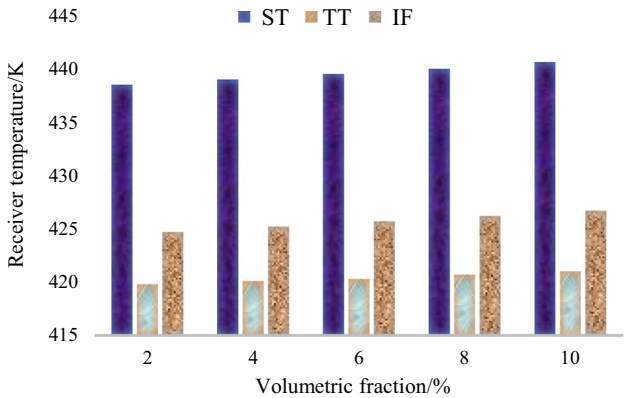

Fig. 11 Variation in receiver temperature of the examined cases at $T_{in}=400$ K

Figure 12 depicts the effect of increase in the nanoparticle concentration on the pressure drop of three considered tubes. This is very crucial parameter as it determines the pumping work, and its higher value makes the performance of overall system lower due to the pressure losses. The results of the given figure show that smooth tube has very less amount of pressure losses as compared to the other two tubes. Pressure drop reduces by increasing nanoparticle concentration because of the fact that nanofluid density has inverse relation with pressure drop. Therefore, density increases with nanoparticle concentration but pressure drop will decrease at constant mass flow rate. It is an important finding in the research that requires a careful design, especially for the absorber tubes with twisted tape inserts. Heat transfer coefficient inside the absorber tubes is also evaluated with rise in nanoparticle concentration, and value of h increases slightly in a linear mode as volume fraction of particles is enhanced as in Fig. 13. Absorber tube with twisted tape insert (case 5) shows the higher value of h because the presence of swirls in fluid flow is important determinant that causes its maximum thermal performance. This phenomenon decreases the outlet temperature of the receiver, while making mean fluid temperature better. As a result, higher values of heat transfer coefficient are obtained. Moreover, increase in the volumetric fraction tends to rise the thermal conductivity of nanoparticles, and according to Eq. (44), heat transfer coefficient has linear relation with thermal conductivity.

Table 3 Comparison between the efficiencies of case 1 with case 2 and case 3

$\frac{T_{in}-T_{amb}}{G_b}$	Case 1/%		Case 2/%		%Age error		Case 3/%		%Age error/%	
	η_{th}	η_{ex}	η_{th}	η_{ex}	η_{th}	η_{ex}	η_{th}	η_{ex}	η_{th}	η_{ex}
0.05	0.7315	0.083	0.7415	0.0915	1.34	9.28	0.7408	0.09	1.25	7.7
0.1	0.7109	0.12	0.7226	0.1295	1.61	7.33	0.721	0.128	1.4	6.25
0.15	0.6824	0.1436	0.6929	0.159	1.51	9.68	0.6912	0.1575	1.27	8.82
0.2	0.6425	0.16	0.6538	0.1789	1.72	10.56	0.6523	0.177	1.5	9.6
0.25	0.605	0.1676	0.6175	0.1885	2.02	11.08	0.6159	0.1874	1.76	10.56
Mean					1.64%	9.58%			1.43%	8.56%

Conclusions

The objective of the present study is to investigate the performance of LS-2 parabolic trough solar collector with different absorber tube geometries using water-based nanofluid and pure base fluid. The effect of different combination of inlet temperatures as an operating parameter on the exergy losses, exergy destruction, energy and exergy efficiencies, heat transfer coefficient, pressure drop and receiver temperature is investigated. Results of the study show that the modified absorber tube geometries have significant increase in exergy and energy efficiencies compared to the conventional smooth absorber tube geometry. Case 5 (tube with nanofluid and twisted tape insert) is observed to be the best performance indicator among the investigated cases. Exergy destroyed due to pressure drop in absorber tube with case 5 is maximum than the other two cases, but it plays a very minor role in overall exergy loss. Maximum exergy losses are found in conventional smooth absorber tube (case 1). The highest amount of pressure drop and friction factor is associated with the case 5 and case 4, respectively, that gives the highest overall performance. Coefficient of heat transfer and pressure drop in case 5 is almost 98% and 43%, while for case 4 is 103% and 42.3%, respectively. Bejan number value is very close to one, and smooth absorber tube (case 1) has the highest entropy generation ratio as compared to the other absorber tubes. Exergy efficiency, heat transfer coefficient and receiver temperature are slightly enhanced by adding nanoparticles; however, pressure drop is noticed to be reduced. Enhancement in thermal efficiency with case 4 (base fluid with twisted tape) ranges from 1.48 to 1.79%, while case 2 (base fluid with fins) from 1.27% to 1.54%. However, the combination of nanofluid with twisted tape (case 5) and fins (case 3) gives 1.99% to 2.71% and 1.8% to 2.44%, respectively. More specifically, nanofluids show increased thermal properties compared to the respective base fluids so, they are more important applicants for the future of heat transfer applications. Such advantages make them strong heat transfer fluids in high solar thermal applications. However, they have a high viscosity that causes higher-pressure drop and consequently to higher pumping power demand. This limitation is one of the most important issues that need to be taken into account in the system design with nanofluids. The higher-pressure drop is a drawback of the thermal enhancement techniques as it is associated with higher pumping work, which enhances the operating and pumping system investment cost. The main drawback of nanofluids in PTCs is found to be pressure drop increase that can be decreased by optimization in nanoparticles volume fraction and mass flow rate.

Appendix

The appendix section is devoted to the percentage error calculation by considering smooth absorber tube with nanofluid as a reference case, while efficiencies of other two cases (twisted and internal fins with nanofluid) are compared with the reference one (Table 3).

Case 1: Reference case (smooth absorber tube with nanofluid).
Case 2: Twisted tape insert absorber tube with nanofluid.
Case 3: Absorber tube with longitudinal internal fins with nanofluid.

References

1. Kumaresan G, Sudhakar P, Santosh R, Velraj R. Experimental and numerical studies of thermal performance enhancement in the receiver part of solar parabolic trough collectors. Renew Sustain Energy Rev. 2017;77:1363–74.
2. Agrafiotis C, Roeb M, Sattler C. A review on solar thermal syngas production via redox pair-based water/carbon dioxide splitting thermochemical cycles. Renew Sustain Energy Rev. 2015;42:254–85.
3. SalgadoConrado L, Rodriguez-Pulido A, Calderón G. Thermal performance of parabolic trough solar collectors. Renew Sustain Energy Rev. 2017;67:1345–59.
4. Fuqiang W, Ziming C, Jianyu T, Yuan Y, Yong S, Linhua L. Progress in concentrated solar power technology with parabolic trough collector system: a comprehensive review. Renew Sustain Energy Rev. 2017;79:1314–28.

5. International Renewable Energy Agency. Renewable energy technologies: cost analysis series. Section 2, Volume 1: concentrating solar power; 2012.
6. Kline SJ, Mcclintock FA. Describing uncertainties in single-sample experiments. Mech Eng. 1953;75:3–8.
7. Moffat RJ. Describing the uncertainties in experimental results. Exp Therm Fluid Sci. 1988;1:3–17.
8. Kalogirou S. Solar energy engineering: processes and systems. Amsterdam: Elsevier; 2009.
9. Behar O, Khellaf A, Mohammedi K. A novel parabolic trough solar collector model-validation with experimental data and comparison to engineering equation solver (EES). Energy Convers Manag. 2015;106:268–81.
10. Bellos E, Tzivanidis C, Antonopoulos KA, Gkinis G. Thermal enhancement of solar parabolic trough collectors by using nanofluids and converging-diverging absorber tuBE. Renew Energy. 2016;94:213–22.
11. Bellos E, Tzivanidis C, Antonopoulos KA. A detailed working fluid investigation for solar parabolic trough collectors. Appl Therm Eng. 2017;114:374–86.
12. Sandeep HM, Arunachala UC. Solar parabolic trough collectors: a review on heat transfer augmentation techniques. Renew Sustain Energy Rev. 2017;69:1218–31.
13. Ren YT, Qi H, He MJ, Ruan ST, Ruan LM, Tan HP. Application of an improved firework algorithm for simultaneous estimation of temperature-dependent thermal and optical properties of molten salt. Int Commun Heat Mass Transf. 2016;77:33–42.
14. Qiu Y, Li M-J, He Y-L, Tao W-Q. Thermal performance analysis of a parabolic trough solar collector using supercritical CO_2 as heat transfer fluid under non-uniform solar flux. Appl Therm Eng. 2017;115:1255–65.
15. Choi SU, Eastman J. Enhancing thermal conductivity of fluids with nanoparticles. New York: Argonne National Lab; 1995.
16. Basbous N, Taqi M, Janan MA. Thermal performances analysis of a parabolic trough solar collector using different nanofluids. Renew Sustain Energy Conf (IRSEC). 2016. https://doi.org/10.1109/IRSEC.2016.7984006.
17. Coccia G, Di Nicola G, Colla L, Fedele L, Scattolini M. Adoption of nanofluids in low-enthalpy parabolic trough solar collectors: numerical simulation of the yearly yield. Energy Convers Manag. 2016;118:306–19.
18. Ghadirijafarbeigloo S, Zamzamian AH, Yaghoubi M. 3-D numerical simulation of heat transfer and turbulent flow in a receiver tube of solar parabolic trough concentrator with louvered twisted-tape inserts. Energy Proc. 2014;49:373–80.
19. Jaramillo OA, Mónica Borunda KM, Velazquez-Lucho M Robles. Parabolic trough solar collector for low enthalpy processes: an analysis of the efficiency enhancement by using twisted tape inserts. Renew Energy. 2016;93:125–41.
20. Mwesigye A, Bellos-Ochende R, Meyer JP. Heat transfer enhancement in a parabolic trough receiver using wall detached twisted tape inserts. In: Proceedings of the ASME 2013 international mechanical engineering congress and exposition IMECE2013, November 15–21, 2013, San Diego, California, USA.
21. Rawani A, Sharma SP, Singh KDP. Enhancement in performance of parabolic trough collector with serrated twisted-tape inserts. Int J Thermodyn. 2017;20(2):111–9.
22. Diwan K, Soni MS. Heat transfer enhancement in absorber tube of parabolic trough concentrators using wire-coils inserts. Univ J Mech Eng. 2015;3(3):107–12.
23. Ghasemi SE, Ranjbar AA. Numerical thermal study on effect of porous rings on performance of solar parabolic trough collector. Appl Therm Eng. 2017;118(25):807–16.
24. Kumar KR, Reddy KS. Thermal analysis of solar parabolic trough with porous disc receiver. Appl Energy. 2009;86:1804–12.
25. Benabderrahmane A, Aminallah M, Laouedj S, Benazza A, Solano JP. Heat transfer enhancement in a parabolic trough solar receiver using longitudinal fins and nanofluids. J Therm Sci. 2016;25:410–7.
26. Reddy KS, Satyanarayana GV. Numerical study of porous finned receiver for solar parabolic trough concentrator. Eng Appl Comput Fluid Mech. 2008;2(2):172–84.
27. Cheng ZD, He YL, Cui FQ. Numerical study of heat transfer enhancement by unilateral longitudinal vortex generators inside parabolic trough solar receivers. Int J Heat Mass Transf. 2012;55:5631–41.
28. Bellos E, Tzivanidis C, Tsimpoukis D. Multi-criteria evaluation of parabolic trough collector with internally finned absorbers. Appl Energy. 2017;205:540–61.
29. Muñoz J, Abánades A. Analysis of internal helically finned tubes for parabolic trough design by CFD tools. Appl Energy. 2011;88:4139–49.
30. Dudley VE, Kolb GJ, Mahoney AR, et al. Test results: SEGS LS-2 solar collector. Sand Natl Lab. 1994;96:11437.
31. Gnielinski V. New equations for heat and mass transfer in turbulent pipe and channel flow. Int Chem Eng. 1976;16(2):359–68.
32. Incropera FP, Bergman TL, DeWitt DP, Lavine AS. Fundamentals of heat and mass transfer. Wiley;2011.
33. Bellos E, Tzivanidis C, Tsimpoukis D. Thermal enhancement of parabolic trough collector with internally finned absorbers. Appl Energy. 2017;205(June):540–61.
34. Loni R, Asli-ardeh EA, Ghobadian B, Kasaeian AB, Gorjian S. Thermodynamic analysis of a solar dish receiver using different nanofluids. Energy. 2017;133:749–60.
35. Ratlamwala TAH. Abid M. Performance analysis of solar assisted multieffect absorption cooling systems using nanofluids: A comparative analysis. Int J Energy Res; 2018. p. 1–15.
36. Batchelor GK. The effect of Brownian motion on the bulk stress in a suspension of spherical particles. J Fluid Mech. 1977;83(01):97–117.
37. Bellos E, Daniil I, Tzivanidis C. Multiple cylindrical inserts for parabolic trough solar collector. Appl Therm Eng. 2018;143:80–9.
38. Bellos E, Tzivanidis C, Tsimpoukis D. Enhancing the performance of parabolic trough collectors using nanofluids and turbulators. Renew Sustain Energy Rev. 2018;91:358–75.